Title: MRI Diffusion Tensor Tractography to Track and Monitor Peripheral Nerve Recovery after Severe Crush or Cut/Repair Nerve Injury

Date: April 7, 2017

NCT # 02960516

PROTOCOL

BACKGROUND

Relevance

This application is in response to the Neuromusculoskeletal Injuries Research Award (W81XWH-15-JPC-8/CRMRP-NMSIRA) and addresses the following focus areas: i) lack of validated metrics that effectively predict function following neuromusculoskeletal injury and ii) limited number of validated metrics that effectively quantify changes that result from rehabilitation or provision of novel technologies. Specifically, this study seeks to develop a novel MRI-based strategy to monitor nerve recovery after injury and surgical repair in order to intervene in situations where nerves are not recovering appropriately. This project is unique in that is proposes a synergistic collaboration between i) a peripheral neurosurgeon/scientist with expertise in nerve repair and ii) engineers/scientists with expertise in developing and translating advanced MRI approaches for peripheral nerve applications.

Significance

It is estimated that up to 5% of all admissions to level one trauma centers have a peripheral nerve injury [1]. These peripheral nerve injuries may have devastating impacts on quality of life and require months or years to regain function. Neurotmesis, or peripheral nerve transection, is a common injury, with singly cut nerve lacerations accounting for over 60% of the peripheral nerve surgical interventions in civilian studies [2, 3]. For recovery to occur in these patients, axons must grow from the site of repair to the target tissues, a length of up to a meter in humans. By that time, revisional surgery may not be a viable option due to the onset of irreversible muscle atrophy — a transected nerve is estimated to induce a loss of achievable function of approximately 1% for every 6 days of delay [4]. The scenario is even worse for more proximal nerve injuries, such as those that occur in the brachial plexus.

Although nerve transfers can reduce the length of axonal growth required[5], failures still occur and revisions are rarely an option due to the aforementioned delays in detection. Current neurodiagnostics [e.g., electromyography (EMG), nerve conduction studies (NCS)] are of limited utility in severely damaged nerves, providing an incomplete picture of nerve microstructural features until target reinnervation occurs[2, 3, 6]. Thus, physicians are limited to a "wait and watch" approach based on qualitative measures obtained from patient history and/or physical exam. This leads to a suboptimal management of peripheral nerve injuries, which in turn can lead to increased instances of irreversible muscle atrophy, paralysis, and/or formation of painful traumatic neuromas[7].

In terms of the military, extremity injuries accounted for 54% of combat wounds in Operation Iraqi Freedom and Operation Enduring Freedom [8, 9] and recent review of service member injuries during Operation Enduring Freedom noted significant increases in brachial plexus, ulnar, and radial nerve injuries attributable to modern warfare [2, 10-12]. In addition, symptomatic neuroma occurs in 13% to 32% of amputees, causing pain and limiting or preventing the use of prosthetic devices[2, 3, 6]. Take the example of a wounded warrior with a shrapnel injury to his/her elbow, resulting in the loss of an ulnar nerve segment. Even if nerve grafting is performed, true recovery (motor and/or sensory innervation of the hand) could take up to a year under typical circumstances. If the repair fails, which occurs in up to 40% of patients[2, 3, 6], the failure is typically not truly recognized until that year expires using current management protocols. By that time, revisional surgery is typically not a viable option due to the aforementioned onset of irreversible muscle atrophy.

In additional to an inability to effectively monitor nerve recovery after repair, diagnosis of peripheral nerve injuries is difficult using the currently available methods. For example, neurotmesis is a common, but difficult to distinguish, diagnosis following traumatic or iatrogenic extremity injury [13]. Current electrodiagnostic and clinical examinations are invasive, time consuming, and painful. In addition, they cannot perfectly discriminate a severe axonotmetic laceration from a self-resolving neurapraxic injury in the acute setting. This is particularly important in penetrating injuries, or after iatrogenic nerve injuries resulting from nerve blocks, or from intraoperative positioning or external compression, because the degree of axonal injury is unknown.

Electrodiagnostics in Peripheral Nerve Injury

NCS are the current gold standard for defining the severity and distribution of nerve injury in cases of trauma [14-17]. Immediately after a total nerve transection injury, no motor or sensory response will occur across the injured segment, nor will there be any voluntary motor unit potentials (MUPs) from muscles innervated by that nerve. Diminished nerve excitability will be exhibited in 1 to 3 days, along with a gradual reduction in the compound muscle action potential (CMAP) and compound nerve action potential (CNAP) amplitudes in nerves stimulated distally to the region of injury. About 4 to 5 days after injury, absence of CMAP amplitude exists in the motor NCS as well as further reduction in CNAP amplitudes in the sensory NCS. After 6 to 10 days, there is no CNAP response. Positive sharp wave (PSW) muscle potentials are seen at 8 days after nerve injury and fibrillation potentials at 14 days. **This indicates that using EMG and NCS, the complete extent and severity of injury can be assessed adequately only in the third week from injury.** In nerves that are severely injured but not severed, proportional reduction in CMAP and CNAP amplitudes occurs, and needle EMG reveals voluntary MUP in muscles innervated by the injured nerve. In some cases of severe but incomplete nerve injury, initially there are no obtainable voluntary MUPs on needle EMG, usually because of severe nerve injury producing a conduction block. In these cases, a repeat study in 6 to 8 weeks can demonstrate a few small amplitude polyphasic MUPs indicative of reinnervation. **This means that multiple invasive studies over a 2-month course may be required to determine whether surgical exploration is warranted.** Taken together, NCS/EMG offer valuable information, but the studies are invasive, painful, and yield limited information regarding the true nature of the extent of the injury and potential for recovery.

DTI in Peripheral Nerve Injury

Based upon these limitations, there is a significant clinical need in both military and civilian populations need for improved quantitative strategies to assess (and predict) nerve regeneration following surgical repair and in some cases to determine if surgical repair is even indicated. To address this clinical shortcoming, we propose to monitor nerve regeneration following surgery via a magnetic resonance imaging (MRI)-based approach known as diffusion tensor imaging (DTI). Magnetic resonance DTI is an imaging sequence that leverages the anisotropic diffusion of water molecules through axons to visualize neural tracts and assess nervous system pathology [18]. It was chosen for the proposed studies because i) DTI yields quantitative metrics that report in axonal integrity and demyelination [19] and ii) previous work has shown that these metrics are sensitive to peripheral nerve degeneration and regeneration and that that high resolution DTI is capable of detecting sciatic nerve crush injuries [20-24]. Therefore, we hypothesize that acute high resolution DTI measurements of peripheral nerve will be correlated with the degree of axonal injury. **In this proposal, we aim to longitudinally assess DTI in a series of animal and human studies in order to optimize, validate, and translate the ability of DTI to monitor and, more importantly, predict nerve regrowth following trauma and surgical repair. If successful, these DTI strategies could help determine outcomes, predict failures much earlier than current techniques, and even guide re-operation.** They also may have potential for expansion to more proximal, and often devastating, injuries of the brachial plexus.

Peripheral nerve injury is one of the few acute neurologic disorders in which imaging is not standard-of-care. High-resolution ultrasound has shown the ability to accurately identify transected nerves [25, 26]; however, traumatic injuries have proven difficult for diagnosis using ultrasonography due to large hematomas, extensive skin lacerations, edema, and disruption of the normal anatomy [25]. Furthermore, no studies have shown the ability of high-resolution ultrasonography to detect early nerve regeneration, which ultimately would indicate whether additional surgical intervention is required [27]. MR neurography (MRN) [28] describes a group of MRI methods for visualizing peripheral nerves. In the most severe cases of nerve injury involving gaps, MRN is capable of detecting nerve discontinuity; however, over half of all high-grade nerve transections have no gap or minimal gap present [29]. Following structural damage, nerves also exhibit a marked increase in T_2, appearing bright in standard clinical T_2-weighted images (normal peripheral nerve appears nearly isointense with respect to surrounding tissue). Explanations for this change include myelin loss, distortion of axoplasmatic flow, axonal loss, and inflammation[20, 30-32]. Although these signal alterations have been found to be sensitive to the presence of neuropathy, they are inherently qualitative and lack specificity (e.g., they cannot discriminate between myelin and axonal pathologies). In the central nervous system (CNS), quantitative MRI techniques that assay various aspects of myelin and axon pathologies have been developed to alleviate these problems. Of these

quantitative techniques, DTI has been particularly useful in detecting axonal pathologies (e.g., in traumatic brain injury and spinal cord injury [33, 34]).

DTI probes microstructural tissue feature (e.g., axon density) by measuring the effect of tissue barriers on the random diffusion of water molecules [19]. In the absence of boundaries, diffusion is isotropic (i.e., the mean-squared displacement of water molecules is the same in all directions). In tissue, water diffusion is hindered by interactions with various tissue structures (e.g., cellular membranes), resulting in a decreased apparent diffusivity. In peripheral nerve, the ordered arrangement of nerve fibers results in an apparent diffusivity that is lower perpendicular to axons than parallel to them [19], of diffusion anisotropy. In DTI, water diffusion is measured along multiple directions to quantify this diffusion anisotropy. This information can then be used to estimate various DTI parameters, including the mean diffusivity (MD, mean value across all directions), axial diffusivity (AD, diffusivity across axons), radial diffusivity (RD, diffusivity along axons), and fractional anisotropy (FA = 0-1, higher values indicate higher anisotropy). In addition, the primary direction of the fiber bundles along the nerve can be determined from DTI measurements; and fiber tracts can be reconstructed from this information using various fiber tracking methodologies [35].

DTI has been investigated as a tool for monitoring nerve degeneration and/or regeneration in animal models for over twenty years[20-23]. From these studies, it has been established that DTI metrics longitudinally track with electrodiagnostic measures of nerve regeneration as well as functional assessment of recovery. In addition, RD (and FA) values have been shown to correlate with histological measures of axon density during regeneration, while AD values have been shown to correlate with histological measures of demyelination [22]. Thus, DTI is a validated technique for probing nerve regeneration in animal models. Unfortunately, limited data exist on high-grade nerve lacerations and there are is only one acute animal studies of DTI following microsurgical repair (see our *Preliminary Findings* [24]). The studies proposed herein are designed to build upon these previous validation studies and aim to evaluate the ability of DTI to detect nerve repair failure following surgical repair. Once validated, these DTI strategies could potentially predict failures much earlier than current techniques and guide re-operation when possible.

Translation of DTI techniques into human peripheral nerve has lagged developments in animals due, in part, to the technical demands of performing nerve DTI in humans (e.g., the need for high resolution data in clinically feasible scan times). Over the past decade, however, a number of technical developments (i.e., multi-element receive coils, higher field strength clinical systems) have led a number of groups to investigate the feasibility of performing DTI in human peripheral nerves *in vivo*. From these studies, the feasibility of performing DTI of the median nerve [36, 37], ulnar nerve [38], tibial and peroneal nerves [39], and brachial plexus [40] has been demonstrated. With feasibility demonstrated, more recent DTI studies of human peripheral nerve have focused on optimization [41-45] and applications in various neuropathies. Together, these results suggest that DTI metrics can be robustly measured in the distal nerves of the forearm and wrist and are quite sensitive to a number of pathologies (CIDP, GBS, carpel tunnel, trauma) [46-51]. In fact, recent work has shown DTI is sensitive enough to detect preclinical lesions [52] as well as subtle differences between healthy individuals [53]. Additionally, a recent study [53] found that, similar to previous animal studies [22], AD reflects axon integrity and while RD (and FA) reflect myelin sheath integrity in healthy individuals. This suggests that one may be able to individually probe demyelinating and axonal features of various neuropathies with DTI. Despite this large number of peripheral nerve DTI studies in humans, only two case studies[50, 51] have sought to use DTI to monitor nerve regeneration following trauma/surgical repair. These two studies suggest that fiber tracking can detect nerve regeneration as early as 1-2 months in humans (consistent with our preliminary data); however, additional longitudinal data is needed to evaluate the ability of DTI to track and monitor nerve recovery following surgical repair. Therefore, the studies proposed herein aim to longitudinally assess DTI in patients after surgical repair for the first time. DTI measurements will then be compared to currently used electrodiagnostic measurements to determine if DTI can predict failures earlier than current techniques.

Preliminary Findings

We have explored the use of DTI as a modality to assess nerve injury of varied severity, in both ex-vivo and in vivo animal models. We also have preliminary data using DTI to assess nerve injury in humans.

Animal Model Injury Validation

Various degrees of high-grade peripheral nerve injury were evaluated using complete and partial transections of rat sciatic nerves. The severity of nerve injury was predicted at time of surgery with careful microsurgical nerve dissection and verified with histology. During evaluation of the proximal nerve sections, we observed that injured nerves had greater axon caliber than sham nerves (Fig. 1a-b). Completely transected nerves were found to have significantly larger mean axon caliber compared to sham nerves ($p<0.01$; Fig. 1c). As observed in diffuse axonal injury in brain white matter, cytotoxic edema occurs rapidly after damage to the axolemmal membrane causing axonal swelling [54]. We observed that mean axon caliber also scaled with the predicted severity of nerve injury (Fig. 1d), with moderate correlation of predicted percentage of injured axons and mean axon caliber ($r^2=0.60$, $p=0.002$). There was wide variability in axon caliber in nerves predicted to be 75% transected, which we suspect to be due to surgical error. Removing partially transected nerves from the analysis improved the correlation of predicted injury severity and mean axon caliber ($r^2=0.82$, $p=0.0001$).

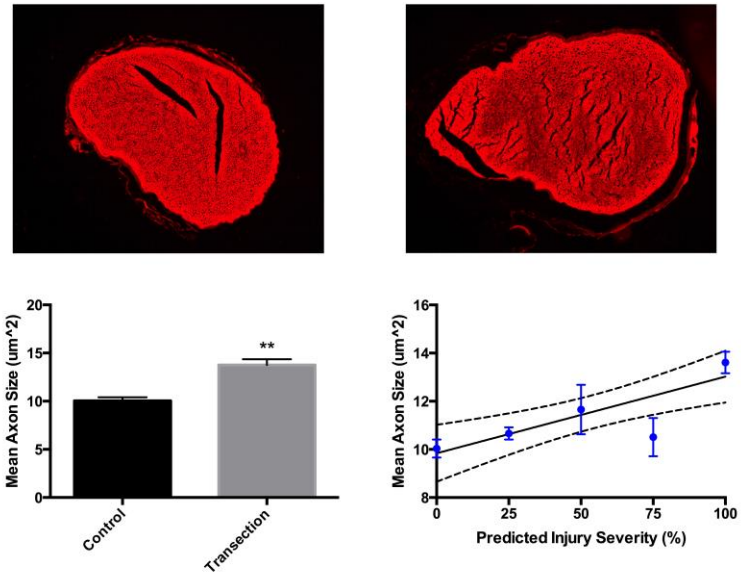

FIG 1. Validation of injury severity by correlation of estimated injury with average axon size in the proximal nerve segment (N=11). Axonal swelling in the proximal segments of transected axons increases the mean axon caliber. Mean axon caliber is linearly correlated to the predicted percentage of transected axons. $^{**}p<0.01$

DTI of Completely Transected Nerves

DTI of excised sciatic nerves were evaluated at three regions-of-interest (ROI) – injury site, 3-mm proximal and 3-mm distal. To prevent partial volume effects, a margin of 100-μm was excluded from the ROI. This also prevented the inclusion of suture material in ROI calculations, since knots are limited to the outermost epineurium. FA, MD and eigenvalues were measured for each ROI (Fig. 2). As expected, the FA was significantly decreased at the injury sites of transected compared to sham rats ($p<0.01$). Although not as strong as at the injury site, the proximal ROI of transected nerves also had lower FA compared to sham rats ($p<0.01$). While the drop in FA at the injury site indicates axonal loss, the proximal ROI changes are most likely due to edema following nerve injury causing an increase in extracellular fluid compartment as well as an increase in axonal edema, which would be expected to decrease FA while simultaneously increasing MD and eigenvalues. Although MD was significantly lower at the injury site ($p<0.01$) and unchanged in the proximal and distal ROIs, the minor eigenvectors showed an increasing trend at all ROIs in transected nerves compared to sham rats (bottom-left panel). Additionally, radial diffusivity, calculated as $RD = (\lambda_2 + \lambda_3)/2$, was significantly increased in the injury site ($p<0.05$) and proximal ROI ($p<0.05$) of transected nerves compared to sham rats. We observed larger variance in distal ROI quantitative measurements, which may be due to variation in fascicular branching at this level in the sciatic nerve. Receiver-operator characteristic (ROC) curves were evaluated for injury-site DTI measurements (bottom-right panel). Injury-site FA produces a near-perfect ROC curve (AUC = 1.000, $p<0.001$), but a larger sample size would be required to prevent type II error.

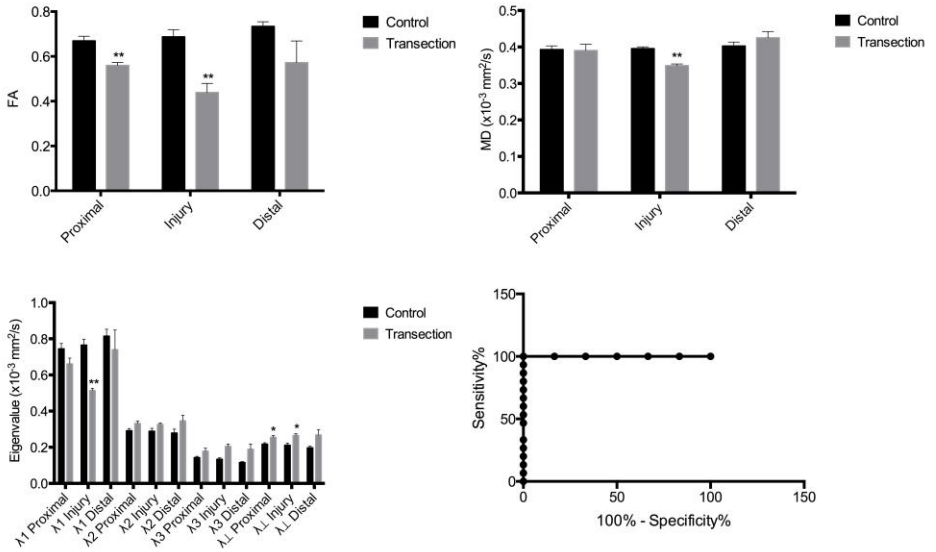

FIG 2. Quantitative analysis of DTI parameters at one hour post-repair in sham and complete sciatic nerve transection injuries from a single imaging session. *p<0.05, **p<0.01

Continuous fiber tractography was performed with a maximum 45° angle and threshold FA of 0.49, corresponding to one standard deviation above the mean FA of all injury sites. Continuous tracts were observed throughout the body of each sham nerve (Fig. 3a), while there were multiple discontinuities present in transected nerves (Fig. 3b), particularly at the injury site. Fewer tracts were visible in the proximal segments of injured nerves, most likely due to reduced FA from tissue edema. Additionally, the number of continuous tracts seeded proximally and passing through the injury site and distal ROI were significantly lower in transected nerves compared to sham rats (p<0.01), (Fig. 3c).

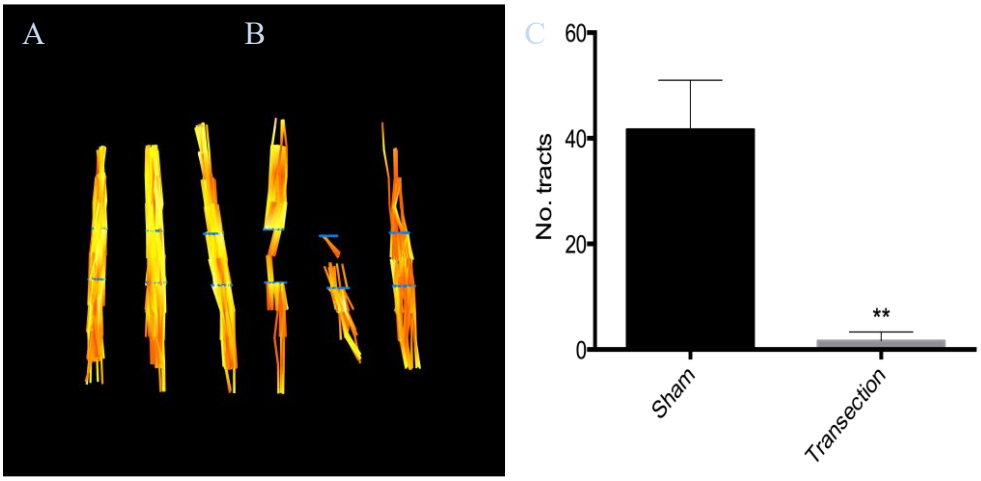

FIG 3. Diffusion tensor tractography in sham (a) and completely transected (b) sciatic nerves. Blue lines indicate seed points for tractography located at 3-mm proximal and distal to the injury sites. Continuous tract counts were significantly lower in transected nerves (c).

DTI of Partially Transected Nerves

For determining the degree to which partial severance of the sciatic nerve could be distinguished with DTI, we imaged partially transected nerves that were graded at the time of surgery as 25%, 50% or 75% nerve severance and validated histologically as described above. DTI parameters were evaluated at the injury ROI for each injured nerve and at the center of each sham nerve (Fig 4a,b). Mean FA was significantly reduced in all injured nerves compared to sham nerves. Mean FA of sham nerves was strongly correlated with the nerve axon count. Minor eigenvalues (λ_2, λ_3) and RD were profoundly increased at all injury sites immediately following injury. This substantial difference could be the result of immediate membrane and myelin disruption present in severance but not contusive nerve injuries. There was a negative correlation between λ2 and radial diffusivity (calculated as $(\lambda_2 + \lambda_3)/2$,) to proximal axon caliber (Fig. 4 c). Since proximal axon caliber correlates with axonal swelling following nerve injury, then this indicates that λ2 and radial diffusivity are inversely proportional to the degree of nerve severance following injury. However, it is likely that there are multiple microstructural factors contributing to these changes.

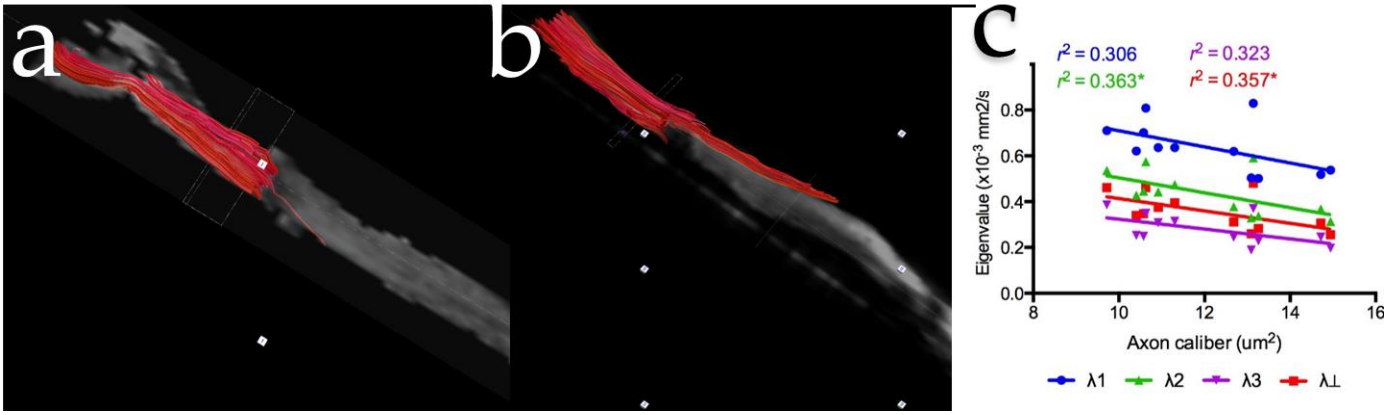

Fig 4. DTI fiber tracking of (a) completely transected and (b) partially transected rat sciatic nerve, demonstrating the sensitivity of the method to controlled degrees of severance injury. (c) Diffusion eigenvalues [AD = λ_1 = along axon, $\lambda_{2/3}$ = across axon, RD = $\lambda_\perp = (\lambda_2 + \lambda_3)/2$] versus proximal axon caliber, which reflects the amount of nerve injury, demonstrating that DTI parameters are inversely proportional to the degree of nerve severance following injury.

DTI of hind limbs

As proof-of-concept, ex vivo imaging was performed on amputated rat hind limbs with sham or complete transection injuries. Tractography was performed with multiple seed points spaced 1 mm apart along the axial length of the sciatic nerve. We found that seeding from a single axial slice as was done in all excised nerves resulted in short tracts, even at low FA thresholds. By seeding from multiple axial slices along the nerve, we were able to capture the length of the nerve while continuing to observe discontinuities at all injury sites (Fig. 5 a-f). Quantitative DTI measurements were calculated at multiple ROIs – injury site, proximal (1-mm, 3-mm and 5-mm) and distal (1-mm, 3-mm and 5-mm). The additional proximal and distal ROIs were included in this analysis to compare effects of surrounding tissue inflammation and edema. Similar to excised nerves, FA was significantly reduced at the injury site of transected nerves ($p<0.01$) and to a lesser extent in the proximal and distal ROIs (Fig. 5g). We hypothesized that external tissue effects should be similar within the entire surgical site, while sciatic nerve injury effects should diminish with increasing distance from the injury site. This was confirmed by our measurements of FA at multiple distances from each injury site (Fig. 5h), in which the FA appears to reach an asymptote at 3-mm, but remains significantly lower than sham animals ($p<0.05$).

Use of DTI in Animal Models to Assess Nerve Repair Outcomes

Our lab monitors electrophysiology such as compound action potentials (CAPs) (Fig 6), histology (Fig 7), and behavioral analysis (Fig 8) to routinely to assess post nerve repair recovery in our rat sciatic model [55-57]. The examples in figure 6 (manuscript in preparation) and [55] (Fig 7,8) focus on our animal studies that have shown that application of a Polyethylene Glycol Hydrogel (PEG) based plasmalemmal sealant to severed peripheral axons can reform the two ends of the cut axons (Fig 6-8) [55-59]. This treatment restores cellular homeostasis and the ability of the sealed axons to conduct electrical signal allowing for early recovery of physiological conduction of sensory and motor impulses and avoiding some of the negative aspects of degeneration and denervation.[58] We note that the early electrophysiologic demonstrations of preserved axonal continuity translate to long term histologic and functional benefits that continue through and beyond 6 wk post-operatively (Fig6-8) [55, 57, 58].

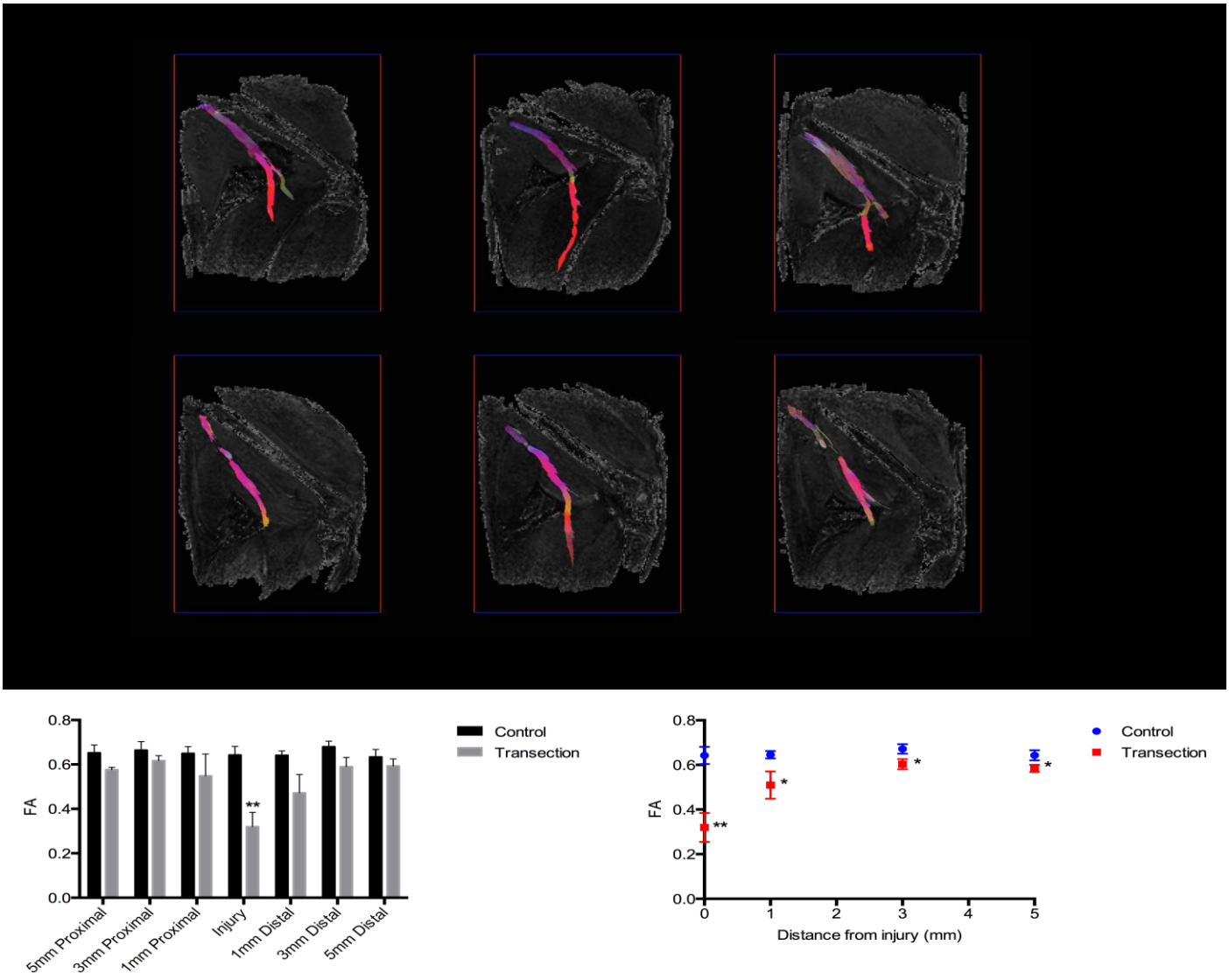

FIG 5. Ex-vivo DTI tractography of rat hind limbs with sham (top panel, top row) and completely transected (top panel, bottom row) sciatic nerves. FA measured at each proximal, injury, and distal ROI is also shown in the two bottom panels.

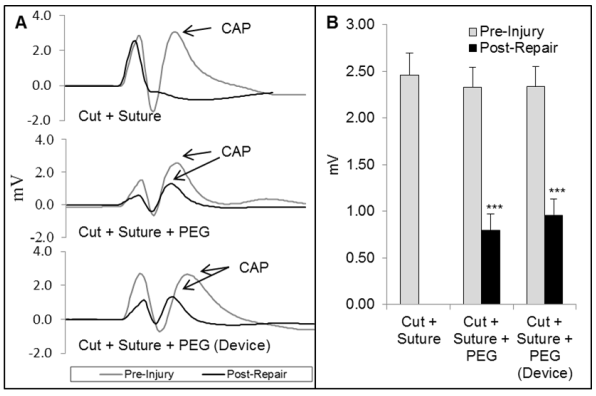

FIG 6. PEG fusion with our device. (a) Representative CAPs recorded pre-injury (gray traces) and post-repair (dark traces) from a control, PEG-fused, and PEG-fused [device] nerve. (b) CAPs (mV, mean ± SE) recorded pre-injury and post-repair for 3 groups: Cut + Suture (n=24), Cut + Suture + PEG (n=24), Cut + Suture + PEG [Device] (n=24). PEG treatment groups demonstrated statistically significant (p<0.001: ***) physiological recovery compared to the "Cut + Suture" group.

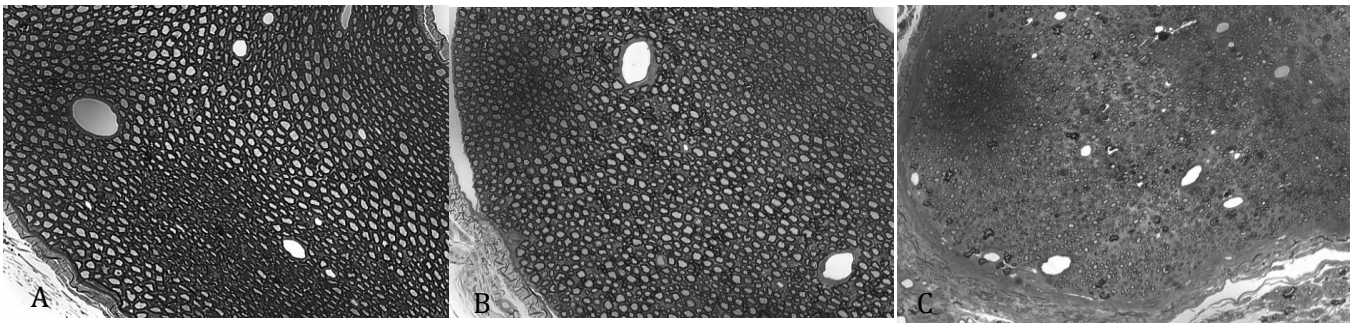

FIG. 7. Plastic embedded toluidine stained sections demonstrating (a) normal nerve, (b) PEG treated allograft for segmental nerve injury, (c) control (no-PEG allograft) distal nerves. For (b) and (c), samples were acquired 6 weeks after repair. Note preserves architecture and lack of scar in the PEG treated nerve allografts.

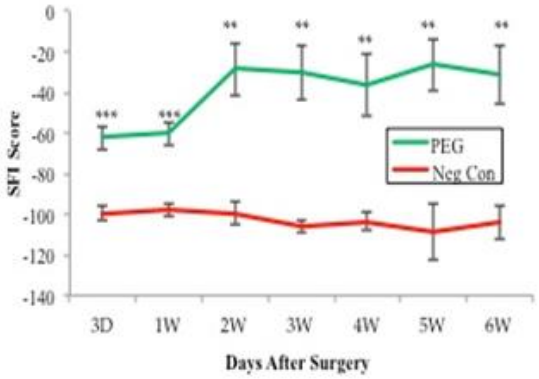

FIG 8. Nerve allograft experiments. SFI (mean ± SE) assessed at 3 days to 6 weeks post-operatively). Red: negative control. Green: PEG 33350-fused. Significance indicated by *p<0.05.

We have employed DTI in the rat sciatic nerve to monitor nerve regrowth following novel PEG fusions (Fig. 9) (manuscript in preparation). **The data shown in figure 9 correlate with electrophysiology, histologic, and behavioral assessments of peripheral nerve recovery implying DTI may be an effective non-invasive technique to monitor nerve repair after repair.** Moreover, we have used PEG fusion in larger animal models such as the porcine model (Fig 10-manuscript in preparation) and DTI demonstrates similar radiographic information regarding axonal continuity.

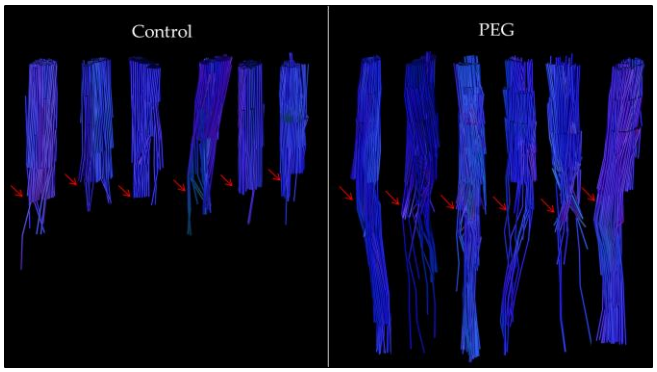

FIG 9. DTI detects variations in axonal continuity. (Left) Fiber tracts (shown top-down in blue for six samples) stop at the severance site (red arrow). (Right) Extended tracts are detected following rat sciatic nerve injury, repair, and subsequent PEG fusion.

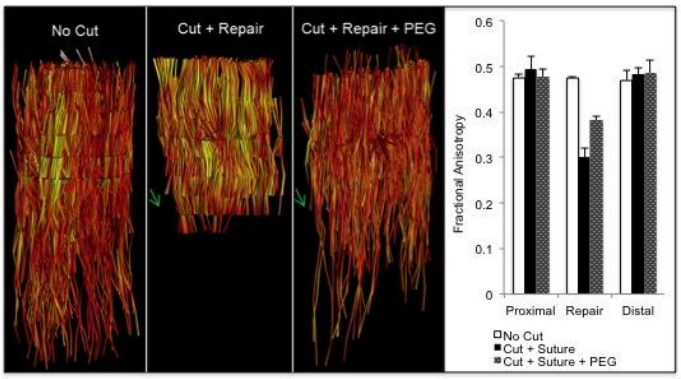

FIG 10. DTI of fixed porcine sciatic nerves harvested immediately following repair. Left panel: Control (left), suture repair (middle), and PEG (right). Green arrows indicate zone of repair. Right panel: FA at the site of injury displayed significant increases between cut repair and PEG groups.

Use of DTI to Assess Human Nerve Repair Outcomes

We have IRB approval for DTI based noninvasive assessment of nerve recovery after upper extremity surgical repair. In preliminary studies, DTI demonstrated total loss of axonal continuity (Fig. 11) and decreased FA distal to the injury site (Fig. 12) of the ulnar nerve after injury with neurotmesis and subsequent surgical repair one week post-op. Moreover, axonal continuity and FA are maintained in the adjacent non-injured median nerve. Serial assessments are planned to determine axonal outgrowth over time. This non-invasive approach is available for our clinic patients where we currently use DTI to detect changes in axonal continuity in the upper extremity of nerve injury (Figs. 11,12).

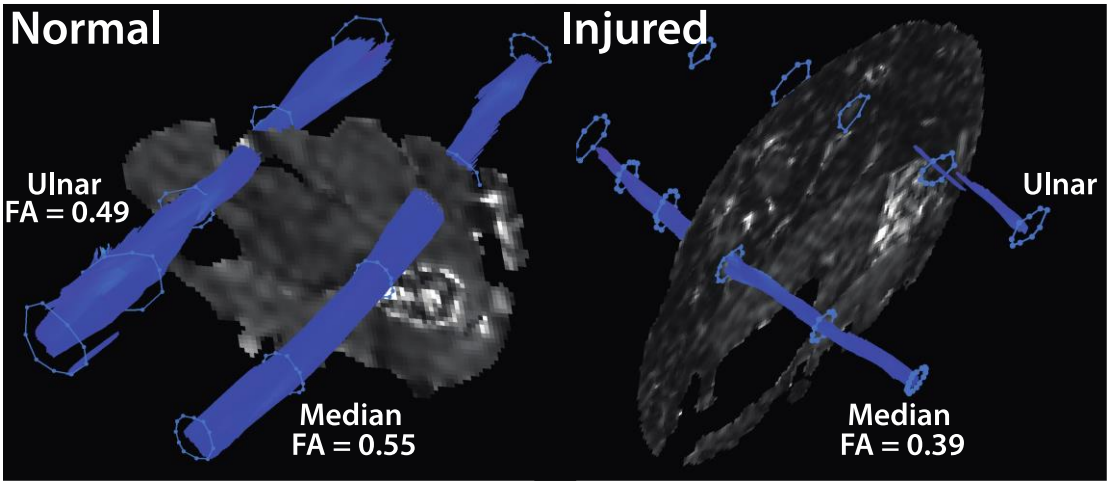

FIG 11. Demonstration of *in vivo* human DTI fiber tracking (fibers in blue) in (left) a control and (right) a patient one week after ulnar nerve injury and repair. Note the decreased mean fiber length in the injured nerve. Legend: MN = median nerve, UN = ulnar nerve.

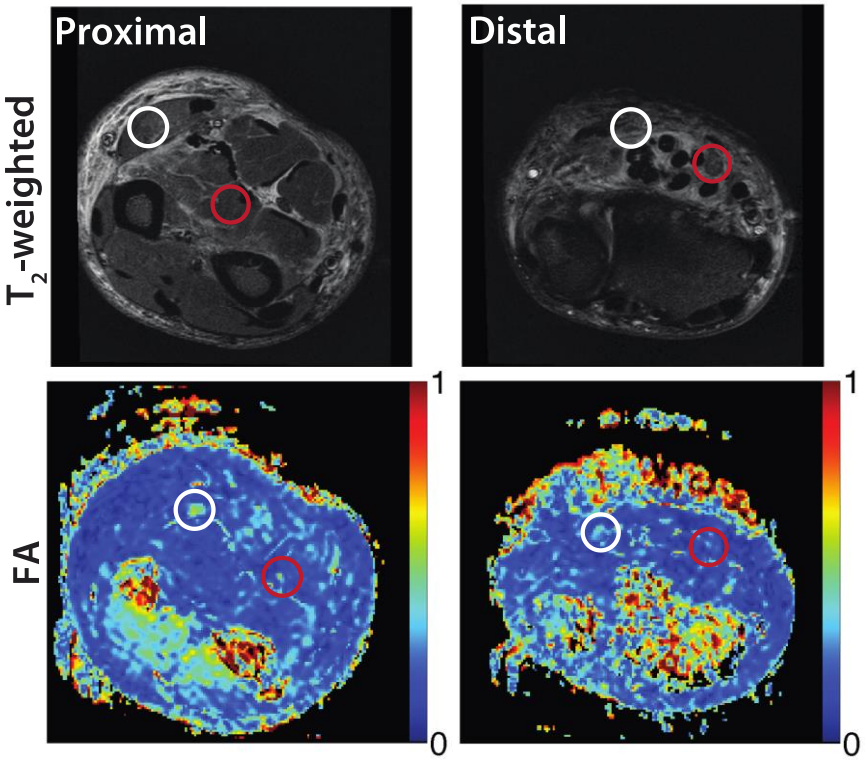

FIG 12. Demonstration of *in vivo* T_2-weightedd anatomical scans and FA maps in a patient one week after ulnar nerve injury and repair. Distal to the injury, decreased FA values were observed in the ulnar nerve (red circles) relative to the median nerve (white circles). Similar FA values were observed in both nerves proximal to the injury.

Summary of preliminary data

Our team has preliminary studies of controlled degrees of severance injury and microsurgical repair found that fiber tracking and DTI indices (e.g., diffusion coefficients along/across axons, or eigenvalues; fractional anisotropy, or FA; mean apparent diffusion coefficient, or ADC) are sensitive to nerve degeneration and injury severity (Fig. 2,3,5) [24]. We have IRB approval for and have shown early success with DTI based assessment after nerve injury and repair in patients with upper extremity nerve injury. We have begun to translate this approach to the clinic where we use DTI to detect changes in axonal continuity in the upper extremity of nerve injury patients (Fig. 11,12). Together, these results demonstrate that i) DTI can be readily performed in the peripheral nerves of animal models and patients with nerve injuries and ii) DTI is sensitive to nerve degeneration/regrowth and injury severity.

Previous Experience

This project proposes a unique collaboration between a peripheral neurosurgeon/scientist (Dr. Wesley Thayer) with expertise in nerve repair and engineers/scientists (Dr. Richard Dortch and Dr. Mark Does) with expertise in developing and translating advanced MRI approaches for peripheral nerve applications. Our laboratories have already collaborated to develop *in vivo* MRI based nerve imaging protocols in both animal models [24] and humans. For the human studies, we share an approved IRB covering post nerve repair MRI of human patients. Data transfer between labs occurs via routine meetings and a shared server. The qualifications and contributions of each of these team members as it pertains to the proposed studies are detailed below.

Wes Thayer (Principal Investigator)

Wesley P. Thayer, MD/PhD is an Assistant Professor of Plastic, Orthopedic Surgery, and Biomedical Engineering. His role in this project is to provide clinical expertise and applicability. He is the primary hand surgeon for the Plastic Surgery Service at Vanderbilt, Chief of Plastic Surgery at the Nashville Veterans Hospital, and maintains a funded basic science laboratory devoted to nerve repair. He has eight peer-reviewed publications focusing on nerve repair using animal models of peripheral nerve injury (see biosketch).

The Vanderbilt Medical Group performed over 372 pure sensory nerve repairs in 2010 and an additional 50 repairs involving mixed nerve loss in the upper extremity. Dr Thayer would have direct access to at least ½ of these repairs. Given this, for the each cohort, sensory, motor, mixed, we anticipate a study recruitment duration less than 24 months to allow 12 month follow up. Patient recruitment will continue until 24 are included and follow up will be for minimum 12 months. For the control cohort requiring we anticipate total study duration less than 24 months and follow-up for at least 12 months. Patient recruitment will continue until 24 are included (approximately 24 months) and follow up will be for 12 months. Assuming a 40% failure rate, this would give us 14 responders and 10 non-responders. Given that we expect to be able to recruit 10-20 patients/year for each group: (sensory, motor, mixed), we expect to reach this target within the 1st 2 yr-year period of this award, allowing for a 6-12 month follow up for all patients. Given our # of patients seen- all patients should be recruited within the first 2 years of the study.

Richard Dortch (Collaborator)

Dr. Richard Dortch, PhD is an Assistant Professor of Radiology and Radiological Sciences, Biomedical Engineering, Vanderbilt University. His role in this project is to provide technical expertise for the human DTI studies. He is currently funded to develop, translate, and validate quantitative MRI measures of peripheral nerve pathology and function in humans. As part of this funding, his lab has developed DTI protocols for the nerves of the wrist, which will serve as the basis for the proposed human imaging studies. He has published multiple peer-reviewed articles directly related to the development of quantitative MRI techniques for applications in the human neuromuscular system; and has extensive experience in developing and translating quantitative MRI techniques into clinical populations (see biosketch).

Mark Does (Collaborator)

Dr. Mark Does, PhD is a Professor of Biomedical, Electrical, and Radiology and Radiologic Sciences at Vanderbilt University. His role in this project is to provide technical expertise for the animal/tissue DTI studies. His lab focuses on the characterization of neural tissue and skeletal muscle with MRI using relaxation,

magnetization transfer, and diffusion as well as compartmental modeling of water proton relaxation and diffusion. He has published over 15 peer-reviewed articles focusing on MRI-based neural imaging (see biosketch). More specifically, he has significant experience and expertise in performing diffusion studies in animal models and serves as the director of Vanderbilt University's Center for Small Animal Imaging.

OBJECTIVE/SPECIFIC AIMS/HYPOTHESIS

The overall objective of these studies is to evaluate the ability of DTI to monitor and, more importantly, predict nerve regrowth following crush or cut with surgical repair. Animal studies will be performed with DTI results compared to measures of axonal recovery from electrophysiology and histology; and validated protocols derived from these animal studies will be translated into humans. We hypothesize that the additional information available via DTI will improve our ability to monitor and predict nerve regrowth following surgical repair or severe crush injury, guiding clinical management either toward or away from surgical intervention.

To accomplish this objective, we have set forth the following aims:

1. Determine if DTI fiber tracking can predict recovery of peripheral nerve function after crush or cut/repair peripheral nerve injury with repair in a rat sciatic nerve model. Graded injuries to either sensory, motor, or mixed nerves will be separately evaluated. Nerve conduits and grafts will be compared to standard repair.
2. Determine if our DTI fiber tracking protocol can predict recovery of peripheral nerve function in human case studies (crush or cut with repair). Pure sensory, motor, and mixed nerve injuries will be evaluated.

RESEARCH STRATEGY

Aim 1: Task 1: Determine if DTI fiber tracking can predict recovery of peripheral nerve function after crush or cut/repair peripheral nerve injury with repair in a rat sciatic nerve model sensory, motor, or mixed nerves will be separately evaluated. Task 2: Graded mixed nerve injury recovery will also be evaluated. Task 3: Finally, nerve conduits and grafts will be compared to standard repair.

Task 1: The rat sciatic nerve injury model has shown promise in our previously published crush injury DTI studies as well as our preliminary studies of controlled degrees of severance injury and microsurgical repair. sensory, motor, or mixed nerves will be separately evaluated. This model will be utilized in this aim because it allows for a direct comparison of DTI (FA, ADC, diffusion eigenvalues) and tractography (mean fiber length) metrics to gold-standard histological measures of pathology as well as electrophysiological and behavioral testing, making it an ideal test-bed to optimize and validate our proposed methods. In this model, we will evaluate a sensory, motor, and mixed nerve injury with crush or cut/repair of the rat sural (sensory), fibular/peroneal (mostly motor) distal to the takeoff of the lateral sural cutaneous, and proximal sciatic (mixed) models, respectively. In each animal group, electrophysiological, histological (toluidine blue), immunohistochemical (motor and sensory specific staining with choactase versus acetylcholine esterase), and behavioral assessment of function with SFI analysis will be performed on day 7, 14, 28, and 3 mo. We will compare predicted outcomes from early time points to actual outcomes to validate *ex vivo* DTI fiber tracking. An *in vivo* MRI will be correlated with an *ex vivo* nerve MRI in a subset of animals to ensure that *ex vivo* results are representative of *in vivo* results. MRI studies will be performed on our 4.7 T 31-cm horizontal bore Agilent DirectDrive scanner (Agilent Technologies, Santa Clara, CA) using a 38-mm Litz quadrature coil (Doty Scientific, Columbia, SC) for RF transmission and reception. This instrumentation is housed in our institute's Center for Small Animal Imaging. High-resolution DTI data will be acquired using a 3D diffusion-weighted spin-echo sequence. Diffusion-weighted data will be acquired in 6 directions ($b = 2000$ s/mm^2) along with a non-diffusion-weighted reference scan; and DTI/fiber tractography parameters will be estimated from these data using standard methods.

Sprague-Dawley rats will be anesthetized and have their left sciatic nerve exposed, after recording compound action potentials (CAPs), the nerve will then be bluntly dissected free. Baseline CAPs will be obtained prior to nerve transection using a Powerlab Acquisition System (ADI; Colorado Springs, CO). One dual terminal nickel electrode will be attached to the proximal and distal end of the nerve prior to its injury

using micromanipulators. One set of terminals will stimulate the sciatic nerve axons and the other terminal will record compound action potentials (CAPs). EMG's pre- and post-injury to the gastrocnemius muscle will also be performed. For the crush group, a hemostat will be applied to the nerve for 10 seconds. For the cut/repair group, an iris scissor will be used to completely transect the sciatic nerve at one point. Microsurgical repair will be performed with 9-0 nylon. Care will be taken to use epineural vasculature as a landmark to maintain fascicular alignment. Control animals will undergo nerve exposure, but no actual crush or cut injury, in order to ensure that the effects noted are due to actual axonal disruption, not inflammation or edema.

For Task 2, Graded mixed nerve injury recovery will also be evaluated. For partial transections, a 3-D printed nerve cutting guide will allow graded transections of 25%, 50%,and 75%. Controls of 0% and 100% mixed nerve crush or cut injury will be from Task 1. Sacrifice will be on day 7, 14, 28, and 3 months. Histologic, MRI, and behavioral testing will occur as in described for Task 1.

For Task 3, nerve conduits and grafts will be compared to standard repair. In the Nerve graft group, a 1 cm section of nerve will be cut from the rat sciatic nerve, reversed, and a microsurgically repaired with 9-0 nylon. A separate group will have a commercially available biologic conduit repair of a 1-cm nerve gap performed microsurgically. Sacrifice will be on day 7, 14, 28, and 3 mo. Histologic, MRI, and behavioral testing will occur as in Task 1.

Outcomes of our nerve repairs will be evaluated based on 1) the extent of Wallerian degeneration using histology, 2) the function of individual nerve fibers using both electrophysiologic assessment (CAPs and EMG) and 3) functionality of the nerve using behavioral testing. We plan to sacrifice rats at 7, 14, 28, and 28 days postoperatively. These rats will undergo behavioral testing at day 7, 14, 28, and 3 months (prior to sacrifice), and then be anesthetized for CAP analysis before the nerve harvested for histologic analysis including toluidine blue analysis (Fig 7). The nerves will also be stained for carbonic anhydrase 2 and cholineacetyltransferase, which label sensory and motor neurons respectively (Fig 6) [60, 61]. After immunohistochemical staining, axons will be counted to determine the number of motor and sensory axons proximal to and distal to the coaptation site. An additional set of animals will undergo MRI-based DTI fiber tracking.

Behavioral testing, consisting of a modified foot fault test and sciatic functional index will be recorded before the injury/repair and on post procedure days 1,2,3, & 7 and weekly thereafter. These are commonly used behavioral methods reported in the literature.[62] At each time point, an unpaired t-test will be used to compare differences in modified foot fault tests, sciatic functional indices, and axon counts between treatment and control groups. ANOVA analysis will be conducted to compare treatment and control levels over time.

Animal statistics: In our previous short term experiments we demonstrated a > 50% change in axon counts using DTI assessment (manuscript in preparation) after nerve injury in our sciatic nerve injury model (Figures 3) [24] with a standard deviation of approximately 15%. If we estimated the benefit in this aim to be 25% with the same standard deviation, using 6 control and 6 experimental animals in each group would allow us to determine a 2 tailed significance of .05 with a power of .87. Groups will be assessed, with rats to be sacrificed at 7, 14, 28days, and at 3 months.

Animal Number's: For Task 1, 6 rats are needed for histology, and 6 for MRI. Therefore, 12 per group will be sacrificed on 4 separate dates (= 48 rats per group). With 7 total groups (control=sham surgery, cut mixed, cut sensory, cut motor, crush mixed, crush motor, crushed sensory), this requires 336 rats total.

For Task 2, graded mixed nerve injury recovery will also be evaluated. For partial transections, a 3-D printed nerve cutting guide will allow graded transections of 25%, 50%,and 75%. Controls of 0% and 100% mixed nerve crush or cut injury will be from Task 1. Again, we will use 12 rats per group, sacrificed on 4 separate dates, for a total of 48 rats per group (= 3 graded transections*48 = 144 total additional rats).

For Task 3, two additional groups will be added: autograft and conduit repair. Again, we will include 12 rats per group, sacrificed on 4 separate dates, for a total of 48 rats per group (= 2 different repairs*48 = 96 additional rats).

For all Tasks, a total of 576 rats will be required.

Aim 2: Determine if DTI fiber tracking can predict recovery of peripheral nerve function in human case studies (crush or cut with repair). Pure sensory, motor, and mixed nerves will be evaluated.

Using the studies from Aim 1 as model of failed nerve recovery, human *in vivo* MRI case studies will be performed. DTI data will be collected at 1, 3, 6, and 12 months after injury and surgical repair. The first time

point was chosen to allow for inflammation to subside, which can confound DTI-based estimates of nerve regeneration (edema can result in increased diffusivities that can be incorrectly interpreted as changes in myelination and/or axonal integrity [63]). We expect that changes due to degeneration/regeneration will be detectable via DTI at this time, as previous case studies noted detectable differences as early as 1 month [50, 51] (as well as our preliminary data in Figs. 11,12). The final time point of 12 months was chosen to allow adequate time for nerve regeneration. This will yield a ground truth assessment of the success of the repair at the end of the study. DTI results will be correlated with results from nerve conduction and EMG studies if clinically indicated acquired at the 3-, 6- and 12-months after surgery. **We hypothesize that DTI will be able to stratify patients that are recovering versus patients with failed repair at earlier times points than nerve conduction and EMG**. An outline of the study in shown in Figure 13.

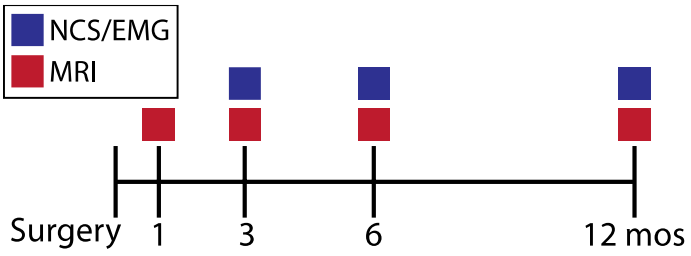

FIG 13. Study design timeline following surgical repair. MRI will be performed at 1, 3, 6, and 12 months after surgery to estimate DTI parameters. NCS/EMG data will be collected for comparison at 3, 6, and 12 months.

Patient Population

Based on designs from previous clinical trials that assessed nerve function, we plan to enroll patients with Sunderland Class V (transection) injuries of injury that will undergo nerve repair. Additional patients with pure motor or sensory injuries will also be investigated. In all patients, complete nerve transection will be verified at the time of the surgery. Upper extremity injuries from the mid-forearm and distal will be eligible. This patient population is considered optimal due to the frequency of occurrence of extremity nerve injuries, the seriousness of the impairment when there is an insensate finger and or lack of intrinsic hand muscle function, and the availability of objective computerized mechanisms to assess outcome.

Inclusion criteria: We will consider subjects between 18 and 64 years old that are diagnosed with a Sunderland Class 5 traumatic neuropathy (transection injury) of upper extremity nerves that require repair. We plan to enroll only patients that have the preceding injury that are deemed candidates for immediate operative repair of this injury and do not have significant medical comorbidities precluding immediate operative intervention. Additionally, patients must be willing to comply with all aspects of the treatment (post-operative visits, occupational therapy) and evaluation schedule over the following 12 months. We plan to include subjects who have peripheral nerve injuries that are complicated by significant vascular or orthopedic damage.

Exclusion criteria: Patients will be excluded from enrollment if their injuries exhibit gross contamination, in circumstances where soft tissue coverage is inadequate, or when staged repair is planned. We will also exclude patients that are diabetic, have been diagnosed with a neuromuscular disease, or are undergoing chemotherapy, radiation therapy, or other treatments known to affect the growth of the neural and vascular system. We will exclude all patients currently enrolled in another investigational study or those who are unlikely to complete the normal regime of occupational therapy. For safety reasons, all pregnant women or women who are breast-feeding will also be excluded from this study along with subject with any ferromagnetic objects that cannot be removed (cardiac pacemakers, aneurysm clip, etc.), and/or a history of claustrophobia. All subjects will undergo a standardized MRI metal screening prior to each MRI scan, and signed consent will be obtained prior to all examinations.

Sample size: Previous optimization DTI studies in human median nerves reported mean (±SD) FA values of 0.7± 0.04 [42]. We do not have human longitudinal data from which we can estimate an effect size; however, Takagi et al. [22] performed ex vivo DTI in a rat injury model longitudinally and reported mean FA values of 0.5 following trauma (FA values are preserved across fixed and in vivo tissue [64]). We, therefore, assume a similar mean FA value after surgery (0.5) with a SD taken from the aforementioned human optimization study (0.04) for our power analysis below. A conservative goal is to detect a 10% increase in FA from this decreased value to stratify successful from unsuccessful surgical interventions. If we test for

differences between these cohorts via a two-tailed pooled Student's t-test ($p = 0.05$), 24 patients would yield a study power of 0.8. Thus, assuming a failure rate of 40%, we will scan 24 patients, approximately 14 of which should have successful surgeries and 10 of should have unsuccessful surgeries.

Subject recruitment: Patients will be recruited through consultations to the hand service at VUMC. Patients scheduled to receive nerve repair procedures meeting the criteria will be considered for participation. All patients must give informed consent prior to any study procedures. In the case of patients who are not competent to make a decision regarding study participation, they will be excluded from the study. A copy of the signed study consent document and authorization forms will be given to each patient. All signed consent documents will be stored in a locked cabinet in the office of the research coordinator or Principal Investigator, S-2221 Medical Center North. In an average year, the Vanderbilt Medical Group performed over 372 digital nerve repairs and an additional 50 repairs involving mixed nerve loss in the upper extremity. As a result, we anticipate reaching our target recruitment of 24 mixed injury subjects within approximately 18 months, leaving adequate time for sequence development in the early stages of the award (1st six months) and 12-month follow-up scan in the latter stages of the award (3rd year). It is rare to see a pure motor nerve injury (ulnar motor branch of the hand). These ulnar motor branch injuries will be additionally included through the duration of the study, but it is unlikely that more than 10 will be observed in a single center study.

Investigational Procedure

After inclusion criteria are met, a standard peri-operative anesthesia evaluation will be undertaken. If the patient is deemed to be of appropriate operative risk to undergo immediate operative repair, informed consent will be obtained and patients will be enrolled in the study. These determinations and obtainment of informed consent will be by research coordinator or principal investigator. It is anticipated that patients will be enrolled primarily through the emergency and trauma units. Clinical testing will occur as scheduled in Table 1. EMG/NCS will be performed after injury if clinically indicated, and at 1,3,6, and possibly 12 months after injury. These studies will be limited to focus on the injured nerve to decrease exam time and discomfort. If patients have fully recovered clinically, additional EMG's will not be performed.

No surgical details will deviate from the current standards for operative repair. All wounds will be closed in the fashion deemed appropriate by the operating surgeon. In essence, the only deviation from the expected surgical repair of these injuries will be post-operative monitoring after nerve repair.

Follow Up: Postoperatively, we plan to follow each patient for a total duration of 12 months after repair, anticipating follow up at 1 week, 1 month, 3 months, 6 months, and 12 months post injury. The data to be collected at each visit are shown in **Table 1**.

DTI Acquisitions

Both arms will be scanned in each subject, with data from the uninjured arm serving as an internal control in each patient. Participants will be imaged in the prone position with the arm being imaged extended over the head. Upon completion of the MRI protocol in the 1st arm, participants will be repositioned with the other arm above the head; and the same MRI protocol will be performed in the 2nd arm. To minimize discomfort, the total protocol duration (DTI scans plus additional calibration scans, scout images, T_1-weighted anatomical, and T_2-weighted anatomical protocols) will be less than 30 minutes for each arm.

Human MRI studies will be performed on our 3.0-Tesla Philips Achieva whole-body MR scanner (Philips Healthcare, Best, The Netherlands). A two-channel body coil will be used for excitation, while a multi-element extremity coil will be used for signal reception. We currently have an array of multi-element coils that allow us to perform studies of both distal nerves of the arm. The details of the DTI protocol will be informed from the animal studies and will be optimized during the initial phase (6 months) of this study in healthy subjects. As a starting point, we will rely on previous DTI optimization studies in human median nerve [44], which employed a multi-slice diffusion-weighted spin-echo sequence with the following parameters: number of diffusion directions = 15, b = 1000 s/mm^2, TR/TE = 8000/52 ms, in-plane resolution = 1.0 x 1.0 mm^2, field-of-view = 80 x 80 mm^2, number of slices = 25, slice thickness = 4 mm, numbers of signal averages = 4, SENSE acceleration factor = 2, and SPAIR fat suppression. Using this protocol, DTI data can be acquired in approximately 10 minutes, leaving adequate time to complete the entire protocol for each arm within 30 minutes.

Table 1. Demographics and Outcome Variables and follow up for nerve injury patients.

Data Recorded	Study Entry	Postoperative Day				
Demographics		1	30	90	180	360
Age	X					
Sex	X					
Race	X					
Medical Comorbidities	X					
Surgical History	X					
Social History	X					
Worker's Compensation Status	X					
Occupation	X					
Concurrent Injuries	X					
Laboratory Values	X					
Rehabilitation Regimen			X	X	X	X
Affected Limb Physical Examination	X	X	X	X	X	X
Normal Limb Physical Examination	X		X	X	X	X
Distance from Injury to Finger Tip	X					
Outcome Variables						
Pain Assessment	X	X	X	X	X	X
Medical Research Council Classification	X	X	X	X	X	X
Data Recorded	Study Entry					
Outcome Variables Continued		1	14	30	90	180
Static 2-Point Discrimination	X	X	X	X	X	X
Moving 2-Point Discrimination	X	X	X	X	X	X
Michigan Hand Questionnaire	X	X	X	X	X	X
Grip Strength	M	M	M	M	M	M
Nine hole peg test		M	M	M	M	M
Short Form 12	X	X	X	X	X	X
Dash Questionnaire	X	X	X	X	X	X
Complications		X	X	X	X	X
MRI			X	X	X	X
X = ALL COHORTS, M= MIXED NERVE						

DTI Analysis

In each subject, we will acquire 15 diffusion-weighted (DW) volumes, each sensitized to diffusion along a different direction, along with a non-DW volume as described above. All DTI pre-processing and tensor estimations will be performed via FMRIB's Software Library (FSL) [69]. All volumes will first be coregistered to the non-DW volume using a 3D affine transformation to correct for the effects of motion and eddy currents. If rotations to the data are applied, the gradient table will be rotated accordingly. Then, the diffusion tensor **D** will be calculated using a weighted linear least squares approach. Three eigenvalues and corresponding eigenvectors will be calculated from **D**, defining the diffusivities and principal direction of diffusion, respectively. From this, we will calculate the FA, MD, RD, and AD on a voxel-wise basis. As a reminder, MD represents the mean diffusivity across all directions, AD represents diffusivity parallel to the principal directions of the axons, RD represents diffusivity parallel to the principal directions of the axons, and FA quantifies the degree of diffusion anisotropy. During regeneration, we expect to observe an increase in FA and decrease in MD due an increase in the order and total number of diffusion barriers, respectively. The relative impact of RD and AD on these changes has yet to be established; however, it has been suggested that RD primarily reflects myelination, while AD primarily reflects axonal degeneration/regeneration [22, 53].

The eigenvalues/eigenvectors estimated from **D** will also be used to perform fiber tractography, which will be performed using the ExploreDTI toolbox [70]. Seed regions-of-interest (ROIs) of each nerve will be drawn

in the most proximal slice to seed each fiber tract. FA threshold values and the angulation tolerances determine the limits for the automatic tracking of fibers. Previous work [43] has determined optimal reconstruction parameters for fiber tractography of healthy nerves (FA threshold = 0.2 and maximum angulation tolerance = 10). We will use these parameters as a starting point, noting that adjustments may need to be made in regenerating nerve. Tractography results will be quantified by estimating the mean length of fiber tracts as well as the relative number of fiber tracts that successfully reach ROIs defined in the most distal slice. During regeneration, we expect mean fiber lengths and relative tract numbers to increase.

Statistics

Statistical analyses will be performed using STATA/IC 13.1 (StataCorp, College Station, TX). In controls, tests will performed to evaluate i) the relationship between DTI metrics and confounding variables (age, sex, and BMI), ii) the variability of DTI metrics between nerves and along nerve segments and iii) the repeatability of DTI metrics across scans and raters. In patients, tests will be performed to i) evaluate the ability of DTI to predict failed nerve recoveries at each time point (using evaluations at 12 months as the ground truth) and ii) evaluate correlations between the DTI parameters and EMG/NCS results.

We will first examine the potential confounding influence of BMI, age, and sex on each DTI parameter via multiple linear regression in controls. A Shapiro-Wilk test on the regression residuals will be used to test for normality. For the sake of this proposal, we assume normality and that parametric statistical tests are appropriate. We will employ corresponding non-parametric tests if normality is not observed. The effects of BMI, age, and sex on DTI parameters will quantified via Pearson partial correlation coefficients. To test for variations across nerve and along nerve segments in control subjects, an ANOVA will be performed. If significant variation is observed, post hoc pair-wise comparisons will be performed using a Bonferroni multiple comparison test.

To understand the ability of DTI parameters to provide estimates of nerve regeneration, it is important to first understand the reliability of the acquisition (interscan) and assessment (interrater) methodology. To estimate the interscan reliability, intraclass correlation coefficients (ICC) will be calculated for each DTI metric in the control scan-rescan data. To test for changes in DTI parameters across time, paired t-tests will also performed between each timepoint. Finally, the interscan variabilities of DTI parameters will be estimated via the repeatability coefficient (RC), which is defined as 1.96 times the SD of the mean difference between scans. Analogous analyses will be performed for the inter-rater data, where nerve ROIs will be independently defined in 12 control subject by two trained raters.

Patients will be grouped into “failed” or “successful” cohorts based upon our evaluations at 12 months. All tests below will be performed in three nerve segments of the injured nerve: i) proximal to the injury, ii) at the injury site, and iii) distal to the injury. The percent difference in DTI parameters between injured and non-injured arms will be used in all analyses to control for confounding factors (e.g., age). To evaluate the ability of DTI to predict failed nerve recoveries at each time point, we will perform two sets of test. First, significant difference between “failed” or “successful” groups will be tested (at each time point and nerve segment) via a Bonferroni multiple comparison test. Second, and ROC analysis will be performed to evaluate the diagnostic potential of each normalized DTI parameter at each time point and nerve segment. Finally, to evaluate relationships between DTI parameters and NCS/EMG data (e.g., CMAP), pairwise Pearson correlations and Bonferroni corrected significance values will be calculated.

Potential Pitfalls/Solutions

As previously mentioned, we expect to be able to meet our subject recruitment targets (24 subjects) within the first two years of the award, allowing one additional year for follow-ups. If we encounter recruitment (or retention) issues, we will investigate the feasibility of performing DTI in the digital nerves of the hand, as injury to these nerves is much more common. Our preliminary studies indicate that our DTI protocols have sufficient resolution to robustly perform DTI of the nerves at the level of the wrist. Performing tractography from these larger, more proximal nerves (median and ulnar) to the more distal digital nerves of the hand may also be feasible, and will be investigated if recruitment and/or retention issues are encountered.

In interpreting our DTI results in patients, it is important to consider each DTI metric’s specificity to different pathological processes. Although diffusion metrics are primarily sensitive to axonal integrity, studies

have shown the DTI indices are also sensitive to myelination and inflammation [63, 65]. Given that all of the processes may occur concurrently during nerve degeneration/regeneration, a direct linkage between changes in DTI parameters and nerve recovery may be difficult, especially at the earlier time points when some level of inflammation may be present. Although histological evaluation of these various processes is not feasible in humans, we have a number of validated quantitative measures (EMG, NCS) that, when available, can be used to validate our DTI findings in humans. In addition, we will rely on the proposed validation studies in animal models (Aim I) to better understand the relationship between our DTI observations and underlying pathology.

In addition to interpretation issues, the sensitivity of DTI parameters to the nerve regeneration process in humans in vivo has yet to be assessed. If we encounter sensitivity issues (for example due to the confounding effects of inflammation), we will investigate a multi-parametric approach that includes magnetization transfer ratio (MTR) MRI as a secondary measure. MTR imaging is based upon interactions between hydrogen protons on water molecules, from which the conventional MRI signal is derived, and hydrogen protons associated with solid-like macromolecules (e.g., myelin lipids), which are typically MRI-silent. Previous studies have indicated that i) MTR relates to myelin content changes in peripheral nerves (from either demyelination and/or axonal degeneration/regeneration) [66] and ii) high-resolution MTR maps of the median and ulnar can be readily acquired within clinical feasible scan times [67]. We have previous experience with this technique and have demonstrated that MTR measurements of the proximal nerves of the leg correlate with functional deficits in both demyelinating/dysmyelinating and axonal inherited neuropathies [68].

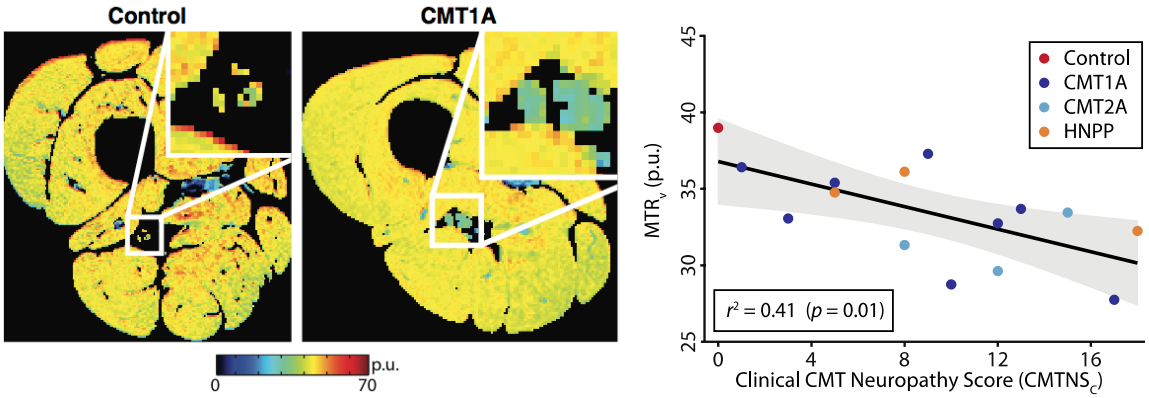

FIG 14. High-resolution MTR maps of the sciatic nerve (zoomed inset) in a control subject and patient with Charcot-Marie-Tooth Type 1A (CMT1A), which is a dysmyelinating inherited neuropathy (left). MTR values in the proximal sciatic nerve correlate with clinical measures of disability (via the CMT Neuropathy score) in both demyelinating/dysmyelinating and axonal inherited neuropahties (right).

SUMMARY

MRI based diffusion tensor tractography has not been previously applied to follow long term recovery in post-surgical animal models or human nerve injuries patients. We have shown early success in post nerve repair animals and we believe the technique will allow clinicians to non-invasively monitor nerve injury patients and predict success, or failure, at a much earlier time point. If this holds true, then this new protocol could change the way nerve injuries are monitored and could help salvage failed repairs and improve overall outcomes. We expect this novel technique will improve the overall rate and extent of recovery after nerve injury. We anticipate that in the future this technique will be broadly useful wherever patients have a nerve injury and are being considered for surgical repair. This includes both soldiers and civilians with nerve injuries from traumatic injury, or after surgical resection for cancer or other reasons.

Timetable for Starting and Completing Each Specific Aim

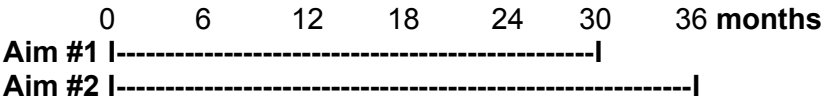
0 6 12 18 24 30 36 months
Aim #1
Aim #2

REFERENCES

1. Noble J, Munro CA, Prasad VS, Midha R. Analysis of upper and lower extremity peripheral nerve injuries in a population of patients with multiple injuries. J Trauma. 1998;45(1):116-22.
2. McAllister RMR GS, Calder JS, Smith PJ The epidemiology and management of upper limb peripheral nerve injuries in modern practice. . J Hand Surg Br. 1996;21:4-13.
3. Wolfe SWH, R.N.; Pederson, W.C.; Kozin, S.H. Green's Operative Hand Surgery. 6th ed. Philadelphia, PA: Elsevier; 2011.
4. Omer GE, Jr. Injuries to nerves of the upper extremity. J Bone Joint Surg Am. 1974;56(8):1615-24.
5. Brown JM, Tung TH, Mackinnon SE. Median to radial nerve transfer to restore wrist and finger extension: technical nuances. Neurosurgery.66(3 Suppl Operative):75-83; discussion Epub 2010/02/04.
6. Mackinnon SE, and Dellon, A. L. Surgery of the Peripheral Nerve. New York: Thieme. 1988:121.
7. Campbell WW. Evaluation and management of peripheral nerve injury. Clin Neurophysiol. 2008;119(9):1951-65. Epub 2008/05/17.
8. Cross JD, Ficke JR, Hsu JR, Masini BD, Wenke JC. Battlefield orthopaedic injuries cause the majority of long-term disabilities. J Am Acad Orthop Surg. 2011;19 Suppl 1:S1-7. Epub 2011/03/17.
9. Stansbury LG, Branstetter JG, Lalliss SJ. Amputation in military trauma surgery. J Trauma. 2007;63(4):940-4. Epub 2007/12/20.
10. Brininger TL, Antczak A, Breland HL. Upper extremity injuries in the U.S. military during peacetime years and wartime years. J Hand Ther. 2008;21(2):115-22; quiz 23. Epub 2008/04/26.
11. Holcomb JB, McMullin NR, Pearse L, Caruso J, Wade CE, Oetjen-Gerdes L, Champion HR, Lawnick M, Farr W, Rodriguez S, Butler FK. Causes of death in U.S. Special Operations Forces in the global war on terrorism: 2001-2004. Ann Surg. 2007;245(6):986-91. Epub 2007/05/25.
12. Fox LC, Kreishman MP. High-energy trauma and damage control in the lower limb. Semin Plast Surg. 2010;24(1):5-10. Epub 2011/02/03.
13. Lee DH, Claussen GC, Oh S. Clinical nerve conduction and needle electromyography studies. J Am Acad Orthop Surg. 2004;12(4):276-87.
14. Chaudhry V, Cornblath DR. Wallerian degeneration in human nerves: serial electrophysiological studies. Muscle Nerve. 1992;15(6):687-93. Epub 1992/06/01.
15. Lee DH, Claussen GC, Oh S. Clinical nerve conduction and needle electromyography studies. The Journal of the American Academy of Orthopaedic Surgeons. 2004;12(4):276-87. Epub 2004/10/12.
16. Oh SJ. Electromyographic studies in peripheral nerve injuries. Southern medical journal. 1976;69(2):177-82. Epub 1976/02/01.
17. Robinson LR. Traumatic injury to peripheral nerves. Muscle Nerve. 2000;23(6):863-73. Epub 2000/06/08.
18. Basser PJ, Mattiello J, LeBihan D. MR diffusion tensor spectroscopy and imaging. Biophys J. 1994;66(1):259-67.
19. Beaulieu C. The basis of anisotropic water diffusion in the nervous system - a technical review. NMR Biomed. 2002;15(7-8):435-55.
20. Stanisz GJ, Midha R, Munro CA, Henkelman RM. MR properties of rat sciatic nerve following trauma. Magn Reson Med. 2001;45(3):415-20.
21. Beaulieu C, Does MD, Snyder RE, Allen PS. Changes in water diffusion due to wallerian degeneration in peripheral nerve. Magn Reson Med. 1996;36(4):627-31.
22. Takagi T, Nakamura M, Yamada M, Hikishima K, Momoshima S, Fujiyoshi K, Shibata S, Okano HJ, Toyama Y, Okano H. Visualization of peripheral nerve degeneration and regeneration: Monitoring with diffusion tensor tractography. Neuroimage. 2009;44(3):884-92.
23. Lehmann HC, Zhang J, Mori S, Sheikh KA. Diffusion tensor imaging to assess axonal regeneration in peripheral nerves. Exp Neurol. 2010;223(1):238-44.
24. Boyer RBK, N.D.; Riley, D.C.;Sexton, K.W.; Pollins, A.C.; Shack, R.B.; Nanney, L.B.; Does, M.D.;Thayer, W.P. 4.7-Tesla Diffusion Tensor Imaging of Acute Traumatic Peripheral Nerve Injury. Journal of Neurosurgery. accepted July 2015.
25. Cartwright MS, Chloros GD, Walker FO, Wiesler ER, Campbell WW. Diagnostic ultrasound for nerve transection. Muscle Nerve. 2007;35(6):796-9.

26. Suk JI, Walker FO, Cartwright MS. Ultrasonography of peripheral nerves. Curr Neurol Neurosci Rep. 2013;13(2):328.
27. Simon NG, Kliot M. Diffusion weighted MRI and tractography for evaluating peripheral nerve degeneration and regeneration. Neural Regen Res. 2014;9(24):2122-4.
28. Howe FA, Filler AG, Bell BA, Griffiths JR. Magnetic resonance neurography. Magn Reson Med. 1992;28(2):328-38.
29. Filler AG, Kliot M, Howe FA, Hayes CE, Saunders DE, Goodkin R, Bell BA, Winn HR, Griffiths JR, Tsuruda JS. Application of magnetic resonance neurography in the evaluation of patients with peripheral nerve pathology. Journal of Neurosurgery. 1996;85(2):299-309.
30. Titelbaum DS, Frazier JL, Grossman RI, Joseph PM, Yu LT, Kassab EA, Hickey WF, LaRossa D, Brown MJ. Wallerian degeneration and inflammation in rat peripheral nerve detected by in vivo MR imaging. AJNR Am J Neuroradiol. 1989;10(4):741-6.
31. Cudlip SA, Howe FA, Clifton A, Schwartz MS, Bell BA. Magnetic resonance neurography studies of the median nerve before and after carpal tunnel decompression. J Neurosurg. 2002;96(6):1046-51.
32. Bendszus M, Wessig C, Solymosi L, Reiners K, Koltzenburg M. MRI of peripheral nerve degeneration and regeneration: correlation with electrophysiology and histology. Exp Neurol. 2004;188(1):171-7.
33. Agosta F, Absinta M, Sormani MP, Ghezzi A, Bertolotto A, Montanari E, Comi G, Filippi M. In vivo assessment of cervical cord damage in MS patients: a longitudinal diffusion tensor MRI study. Brain. 2007;130(Pt 8):2211-9.
34. Bennett RE, Mac Donald CL, Brody DL. Diffusion tensor imaging detects axonal injury in a mouse model of repetitive closed-skull traumatic brain injury. Neurosci Lett. 2012;513(2):160-5.
35. Mori S, van Zijl PC. Fiber tracking: principles and strategies - a technical review. NMR Biomed. 2002;15(7-8):468-80.
36. Kabakci N, Gürses B, Firat Z, Bayram A, Uluğ AM, Kovanlikaya A, Kovanlikaya I. Diffusion tensor imaging and tractography of median nerve: normative diffusion values. AJR Am J Roentgenol. 2007;189(4):923-7.
37. Khalil C, Hancart C, Le Thuc V, Chantelot C, Chechin D, Cotten A. Diffusion tensor imaging and tractography of the median nerve in carpal tunnel syndrome: preliminary results. Eur Radiol. 2008;18(10):2283-91.
38. Jambawalikar S, Baum J, Button T, Li H, Geronimo V, Gould ES. Diffusion tensor imaging of peripheral nerves. Skeletal Radiol. 2010;39(11):1073-9.
39. Hiltunen J, Suortti T, Arvela S, Seppä M, Joensuu R, Hari R. Diffusion tensor imaging and tractography of distal peripheral nerves at 3 T. Clin Neurophysiol. 2005;116(10):2315-23.
40. Vargas MI, Viallon M, Nguyen D, Delavelle J, Becker M. Diffusion tensor imaging (DTI) and tractography of the brachial plexus: feasibility and initial experience in neoplastic conditions. Neuroradiology. 2010;52(3):237-45.
41. Zhou Y, Kumaravel M, Patel VS, Sheikh KA, Narayana PA. Diffusion tensor imaging of forearm nerves in humans. J Magn Reson Imaging. 2012;36(4):920-7. Epub 2012/06/13.
42. Zhou Y, Narayana PA, Kumaravel M, Athar P, Patel VS, Sheikh KA. High resolution diffusion tensor imaging of human nerves in forearm. J Magn Reson Imaging. 2013;39(6):1374-83.
43. Guggenberger R, Eppenberger P, Markovic D, Nanz D, Chhabra A, Pruessmann KP, Andreisek G. MR neurography of the median nerve at 3.0T: Optimization of diffusion tensor imaging and fiber tractography. Eur J Radiol. 2012;81(7):e775-e82.
44. Guggenberger R, Nanz D, Bussmann L, Chhabra A, Fischer MA, Hodler J, Pfirrmann CWA, Andreisek G. Diffusion tensor imaging of the median nerve at 3.0T using different MR scanners: Agreement of FA and ADC measurements. Eur J Radiol. 2013;82(10):e590-e6.
45. Guggenberger R, Nanz D, Puippe G, Rufibach K, White LM, Sussman MS, Andreisek G. Diffusion tensor imaging of the median nerve: intra-, inter-reader agreement, and agreement between two software packages. Skeletal Radiol. 2012;41(8):971-80.
46. Mathys C, Aissa J, Hoerste GMZ, Reichelt DC, Antoch G, Turowski B, Hartung H-P, Sheikh KA, Lehmann HC. Peripheral Neuropathy: Assessment of Proximal Nerve Integrity by Diffusion Tensor Imaging. Muscle Nerve. 2013;48(6):889-96.

47. Kakuda T, Fukuda H, Tanitame K, Takasu M, Date S, Ochi K, Ohshita T, Kohriyama T, Ito K, Matsumoto M, Awai K. Diffusion tensor imaging of peripheral nerve in patients with chronic inflammatory demyelinating polyradiculoneuropathy: a feasibility study. Neuroradiology. 2011;53(12):955-60.
48. Guggenberger R, Markovic D, Eppenberger P, Chhabra A, Schiller A, Nanz D, Prüssmann K, Andreisek G. Assessment of Median Nerve with MR Neurography by Using Diffusion-Tensor Imaging: Normative and Pathologic Diffusion Values. Radiology. 2012;265(1):194-203.
49. Hiltunen J, Kirveskari E, Numminen J, Lindfors N, Goransson H, Hari R. Pre- and post-operative diffusion tensor imaging of the median nerve in carpal tunnel syndrome. Eur Radiol. 2012;22(6):1310-9.
50. Meek MF, Stenekes MW, Hoogduin HM, Nicolai J-PA. In vivo three-dimensional reconstruction of human median nerves by diffusion tensor imaging. Exp Neurol. 2006;198(2):479-82.
51. Kabakci NT, Kovanlikaya A, Kovanlikaya I. Tractography of the median nerve. Semin Musculoskelet Radiol. 2009;13(1):18-23.
52. Baeumer P, Pham M, Ruetters M, Heiland S, Heckel A, Radbruch A, Bendszus M, Weiler M. Peripheral Neuropathy: Detection with Diffusion-Tensor Imaging. Radiology. 2014;273(1):185-93.
53. Heckel A, Weiler M, Xia A, Ruetters M, Pham M, Bendszus M, Heiland S, Baeumer P. Peripheral Nerve Diffusion Tensor Imaging: Assessment of Axon and Myelin Sheath Integrity. PLoS ONE. 2015;10(6):e0130833.
54. Liang D, Bhatta S, Gerzanich V, Simard JM. Cytotoxic edema: mechanisms of pathological cell swelling. Neurosurg Focus. 2007;22(5):E2. Epub 2007/07/07.
55. Riley DC, Bittner GD, Mikesh M, Cardwell NL, Pollins AC, Ghergherehchi CL, Bhupanapadu Sunkesula SR, Ha TN, Hall BT, Poon AD, Pyarali M, Boyer RB, Mazal AT, Munoz N, Trevino RC, Schallert T, Thayer WP. Polyethylene glycol-fused allografts produce rapid behavioral recovery after ablation of sciatic nerve segments. J Neurosci Res. 2015;93(4):572-83.
56. Rodriguez-Feo CL, Sexton KW, Boyer RB, Pollins AC, Cardwell NL, Nanney LB, Shack RB, Mikesh MA, McGill CH, Driscoll CW, Bittner GD, Thayer WP. Blocking the P2X7 receptor improves outcomes after axonal fusion. J Surg Res. 2013;184(1):705-13.
57. Sexton KW, Pollins AC, Cardwell NL, Del Corral GA, Bittner GD, Shack RB, Nanney LB, Thayer WP. Hydrophilic polymers enhance early functional outcomes after nerve autografting. J Surg Res. 2012;177(2):392-400.
58. Bittner GD, Keating CP, Kane JR, Britt JM, Spaeth CS, Fan JD, Zuzek A, Wilcott RW, Thayer WP, Winograd JM, Gonzalez-Lima F, Schallert T. Rapid, effective, and long-lasting behavioral recovery produced by microsutures, methylene blue, and polyethylene glycol after completely cutting rat sciatic nerves. J Neurosci Res. 2012;90(5):967-80. Epub 2012/02/04.
59. Sexton KW R-FC, Boyer RB, Del Corral GA, Riley DC, Pollins AC, Cardwell NL, Shack RB, Nanney LB , Thayer WP Axonal Fusion via Conduit Based Delivery of Hydrophilic Polymers. Hand 2015 accepted for publication.
60. Riley DA, Sanger JR, Matloub HS, Yousif NJ, Bain JL, Moore GH. Identifying motor and sensory myelinated axons in rabbit peripheral nerves by histochemical staining for carbonic anhydrase and cholinesterase activities. Brain research. 1988;453(1-2):79-88. Epub 1988/06/21.
61. Schemann M, Sann H, Schaaf C, Mader M. Identification of cholinergic neurons in enteric nervous system by antibodies against choline acetyltransferase. The American journal of physiology. 1993;265(5 Pt 1):G1005-9. Epub 1993/11/01.
62. Nichols CM, Myckatyn TM, Rickman SR, Fox IK, Hadlock T, Mackinnon SE. Choosing the correct functional assay: a comprehensive assessment of functional tests in the rat. Behavioural brain research. 2005;163(2):143-58. Epub 2005/06/28.
63. Stanisz GJ, Webb S, Munro CA, Pun T, Midha R. MR properties of excised neural tissue following experimentally induced inflammation. Magn Reson Med. 2004;51(3):473-9.
64. D'Arceuil HE, Westmoreland S, de Crespigny AJ. An approach to high resolution diffusion tensor imaging in fixed primate brain. Neuroimage. 2007;35(2):553-65.
65. Beaulieu C, Allen PS. DETERMINANTS OF ANISOTROPIC WATER DIFFUSION IN NERVES. Magn Reson Med. 1994;31(4):394-400.
66. Odrobina EE, Lam TYJ, Pun T, Midha R, Stanisz GJ. MR properties of excised neural tissue following experimentally induced clemyelination. NMR Biomed. 2005;18(5):277-84.

67. Gambarota G, Mekle R, Mlynárik V, Krueger G. NMR properties of human median nerve at 3 T: proton density, T1, T2, and magnetization transfer. J Magn Reson Imaging. 2009;29(4):982-6.
68. Dortch RD, Dethrage LM, Gore JC, Smith SA, Li J. Proximal nerve magnetization transfer MRI relates to disability in Charcot-Marie-Tooth diseases. Neurology. 2014;83(17):1545-53.
69. Smith SM, Jenkinson M, Woolrich MW, Beckmann CF, Behrens TE, Johansen-Berg H, Bannister PR, De Luca M, Drobnjak I, Flitney DE, Niazy RK, Saunders J, Vickers J, Zhang Y, De Stefano N, Brady JM, Matthews PM. Advances in functional and structural MR image analysis and implementation as FSL. Neuroimage. 2004;23 Suppl 1:S208-19.
70. Leemans A, Jeurissen B, Sijbers J, Jones D, editors. ExploreDTI: a graphical toolbox for processing, analyzing, and visualizing diffusion MR data. 17th Annual Meeting of ISMRM 2009.